



# Evaluation of atrial septal defects with 4D flow MRI—multilevel and inter-reader reproducibility for quantification of shunt severity

Raluca G. Chelu<sup>1,2</sup> · Michael Horowitz<sup>3</sup> · Dominica Sucha<sup>4</sup> · Isabella Kardys<sup>5</sup> · Delphine Ingremeau<sup>6</sup> · Shreyas Vasanawala<sup>7</sup> · Koen Nieman<sup>1,2,7,8</sup> · Jean-Francois Paul<sup>6</sup> · Albert Hsiao<sup>3</sup>

Received: 7 March 2018 / Revised: 10 August 2018 / Accepted: 16 August 2018  
© The Author(s) 2018

## Abstract

**Purpose** With the hypothesis that 4D flow can be used in evaluation of cardiac shunts, we seek to evaluate the multilevel and interreader reproducibility of measurements of the blood flow, shunt fraction and shunt volume in patients with atrial septum defect (ASD) in practice at multiple clinical sites.

**Materials and methods** Four-dimensional flow MRI examinations were performed at four institutions across Europe and the US. Twenty-nine patients (mean age, 43 years; 11 male) were included in the study. Flow measurements were performed at three levels (valve, main artery and periphery) in both the pulmonary and systemic circulation by two independent readers and compared against stroke volumes from 4D flow anatomic data. Further, the shunt ratio ( $Q_p/Q_s$ ) was calculated. Additionally, shunt volume was quantified at the atrial level by tracking the atrial septum.

**Results** Measurements of the pulmonary blood flow at multiple levels correlate well whether measuring at the valve, main pulmonary artery or branch pulmonary arteries ( $r=0.885-0.886$ ). Measurements of the systemic blood flow show excellent correlation, whether measuring at the valve, ascending aorta or sum of flow from the superior vena cava (SVC) and descending aorta ( $r=0.974-0.991$ ). Intraclass agreement between the two observers for the flow measurements varies between 0.96 and 0.99. Compared with stroke volume, pulmonic flow is underestimated with 0.26 l/min at the main pulmonary artery level, and systemic flow is overestimated with 0.16 l/min at the ascending aorta level. Direct measurements of ASD flow are feasible in 20 of 29 (69%) patients.

**Conclusion** Blood flow and shunt quantification measured at multiple levels and performed by different readers are reproducible and consistent with 4D flow MRI.

**Keywords** 4D flow MRI · Atrial septal defect · Multiple measurements

**Electronic supplementary material** The online version of this article (<https://doi.org/10.1007/s10334-018-0702-z>) contains supplementary material, which is available to authorized users.

✉ Raluca G. Chelu  
ralucachelu@hotmail.com

- 1 Department of Radiology, Erasmus MC, 's Gravendijkwal 230, Ca207a, 3015 CE Rotterdam, The Netherlands
- 2 Department of Cardiology, Erasmus MC, Rotterdam, The Netherlands
- 3 Department of Radiology, UCSD, San Diego, CA, USA
- 4 Department of Radiology, UMC, Utrecht, The Netherlands

## Introduction

Atrial septal defects (ASD) are one of the most common congenital heart defects with an estimated prevalence of 1.6 per 1000 live births [1]. Most prevalent are ostium secundum defects followed by ostium primum and sinus venosus

<sup>5</sup> Department of Epidemiology, Erasmus MC, Rotterdam, The Netherlands

<sup>6</sup> Department of Radiology, Institut Mutualiste Montsouris, Paris, France

<sup>7</sup> Department of Radiology, Stanford Medical Center, Palo Alto, CA, USA

<sup>8</sup> Department of Cardiology, Stanford Medical Center, Palo Alto, CA, USA

defects [2]. Partial anomalous pulmonary venous connections (PAPVRs) are often associated with ASD, especially with sinus venosus defects. When repaired at a young age, patients with ASD have a life expectancy similar to the general population [3, 4]. Left untreated, patients with large ASD gradually develop pulmonary hypertension, reversal of the left-to-right shunt and eventually right heart failure. In clinical practice, ASD closure is considered for patients with a shunt fraction greater than 1.5 [2].

Multiple imaging modalities are used to detect and delineate these anatomic defects. Transthoracic echocardiography (TTE) is used as a primary screening modality. However, associated pathologies such as PAPVR are more difficult to identify with TTE. When TTE is inconclusive, transesophageal echocardiography (TEE) may be helpful [5]. Alternatively, computed tomography (CT) and magnetic resonance imaging (MRI) are increasingly used.

MRI has shown its incremental value in congenital heart disease (CHD) [6] and ASD in particular [7]. MRI is the gold standard for noninvasive quantification of right heart function and shunt fraction [8, 9]. It may detect intracardiac shunting and additional findings including PAPVR [10]. However, it is performed with numerous breath-holds and relatively long examination times, which may be challenging for cardiac patients.

A promising and rapidly evolving MRI technique is 4D flow imaging, a volumetric, free-breathing acquisition technique of flow velocity data with simultaneous assessment of anatomic structures [11]. The 4D flow MRI allows for flow quantification at any level within the acquired field of view and calculation of cardiac volumes and biventricular function [12–14].

A few studies have evaluated the use of 4D flow MRI for visualization and quantification of cardiac shunts [15–17]. It is not yet clear, however, whether this technique is robust across the range of imaging parameters that might be used in the clinical environment because of differences in body habitus or equipment. In the clinical setting, there may be heterogeneity in imaging techniques because of local preferences or needs for imaging parameters such as the signal-to-noise ratio (SNR), spatial resolution, scanning time, velocity-encoding speed ( $v_{\text{enc}}$ ), available equipment, field strengths (1.5 T, 3 T) and patient body habitus. A previous paper showed that it is possible to measure venous flow even when using high  $v_{\text{enc}}$  [18]. However, uncertainty remains about whether this technique is applicable outside of the research setting. As this technology has recently become more broadly clinically available, we seek to determine in this study whether 4D flow can robustly be used for the evaluation of cardiac shunts at different levels of the vascular tree using 4D flow data acquired across multiple

centers—specifically measurements of the blood flow, shunt fraction and shunt volume.

## Methods

### Study design

Cardiac MRI examinations including 4D flow were gathered from four academic centers in the US and Europe in patients referred for evaluation of ASD between December 2014 and January 2017. In three centers, 4D flow was performed as part of the clinical protocol and retrospectively included in this study. Informed consent was waived by the local IRB. In the remaining center, patients were prospectively enrolled and signed informed consent for an MRI including 4D flow. The study protocol was compliant with Declaration of Helsinki and received approval from each local medical ethics committee.

### 4D flow acquisition

At each center, 4D flow MRI acquisition protocols were optimized based on locally available equipment, medications, and clinical requirements. The retrospectively gated 4D flow acquisition was performed using clinical MRI scanners (69% at 1.5 T, 31% at 3 T) (GE Healthcare, Milwaukee, WI, USA) after administration of a gadolinium-based contrast agent. Scan time ranged between 7.46 and 14.75 min (median 10.75 min). All imaging parameters are presented in Table 1.

### Post-processing

Data were analyzed using dedicated post-processing software (Arterys Inc, San Francisco, CA). Semiautomatic eddy-current correction was applied [19]. Data were visualized, interpreted for the presence of ASD and classified according to type of septal defect. To evaluate consistency of the data across the vascular tree, shunt quantification was performed at multiple levels, as described below. Further, to evaluate intraobserver reproducibility, background correction and measurements were done by two readers independently (with 4 and 1 year of experience with 4D flow).

### ASD visualization and classification

To detect and visualize the ASDs, volumetric data sets were reformatted in multiple orientations using several rendering techniques: color-coded velocity overlay,

**Table 1** Scanning details

	Center 1 ( <i>n</i> =4)	Center 2 ( <i>n</i> =9)	Center 3 ( <i>n</i> =8)	Center 4 ( <i>n</i> =8)	Total ( <i>n</i> =29)
Field strength ( <i>T</i> )	1.5 T (100%)	3 T (100%)	1.5 T (100%)	1.5 T (100%)	1.5 T (69%) 3 T (31%)
Contrast agent	Gadobutrol (100%)	Gadofosveset trisodium (67%), gadobenate dimeglumine (33%)	Gadoterate meglumine (50%), gadobenate dimeglumine (50%)	Gadofosveset trisodium (37%), gadobenate dimeglumine (63%)	Gadofosveset trisodium (14%), gadoterate meglumine (31%), gadobutrol (14%), gadobenate dimeglumine (41%)
Resolution acquired (mm)	(1.8–2.0) × (2.1–2.4) × 2.8	(1.3–2.0) × (1.4–2.4) × (2.4–3.2)	(1.4–1.8) × (2.3–2.8) × 2.6	(1.0–1.8) × (1.4–2.2) × 3.0	(1.3–2.0) × (1.4–2.8) × (2.4–3.2)
Resolution reconstructed (mm)	(1.8–2.0) × (2.1–2.4) × 1.4	(1.3–2.0) × (1.3–2.2) × (1.2–1.6)	(1.4–1.8) × (2.3–2.8) × 1.3	(1.0–1.4) × (1.4–1.8) × 1.5	(1.3–2.0) × (1.3–2.2) × (1.2–1.6)
Temporal resolution (ms) <sup>a</sup>	61.4–62.4	61.2–81.8 <sup>+</sup>	51.6–76.3	49.3–83.2	49.3–83.2
Heart rate	64–72	66–80	55–103	48–77	48–103
Sinus rhythm	100%	100%	100%	75%	93%
Venc (cm/s)	180–200	150–250	200–500	250	150–500
Scanning time (min)	10.42–11.58	10.75–14.75	7.46–14.75	7.46–10.95	7.46–14.75

Values are ranges (minimum–maximum)

*T* Tesla, *HR* heart rate, *venc* velocity encoding value

<sup>a</sup>In four patients, data were not available

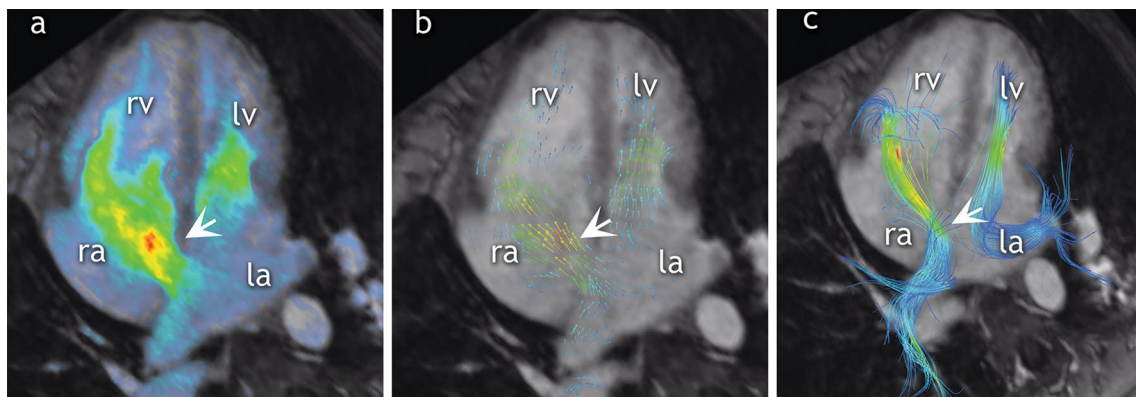


**Fig. 1** Multiple rendering techniques for ASD visualization. Color velocity overlay helps to identify the shunt in a frame-by-frame approach, but does not show flow directionality **a**. Flow direction is emphasized with vector overlay **b**. Streamlines help to track the flow

that comes from pulmonary veins to the left atrium. In case of an atrial septum defect, the blood will cross to the right atrium and right ventricle. *Ra* right atrium, *rv* right ventricle, *la* left atrium, *lv* left ventricle, *SVC* superior vena cava

vector-velocity overlay, and streamlines (Fig. 1). ASDs were classified according to international guidelines [2, 5]. To visualize primum and secundum ASDs, the atrial septum was examined in short and long axis (Supplementary Fig. 1). Furthermore, to evaluate the presence of sinus

venosus ASD, the superior and inferior cavo-atrial junctions were visualized. The coronary sinus was carefully assessed for detection of unroofed coronary sinus (Supplementary Fig. 2). In addition, streamlines were created from regions of interest in the pulmonary veins to further

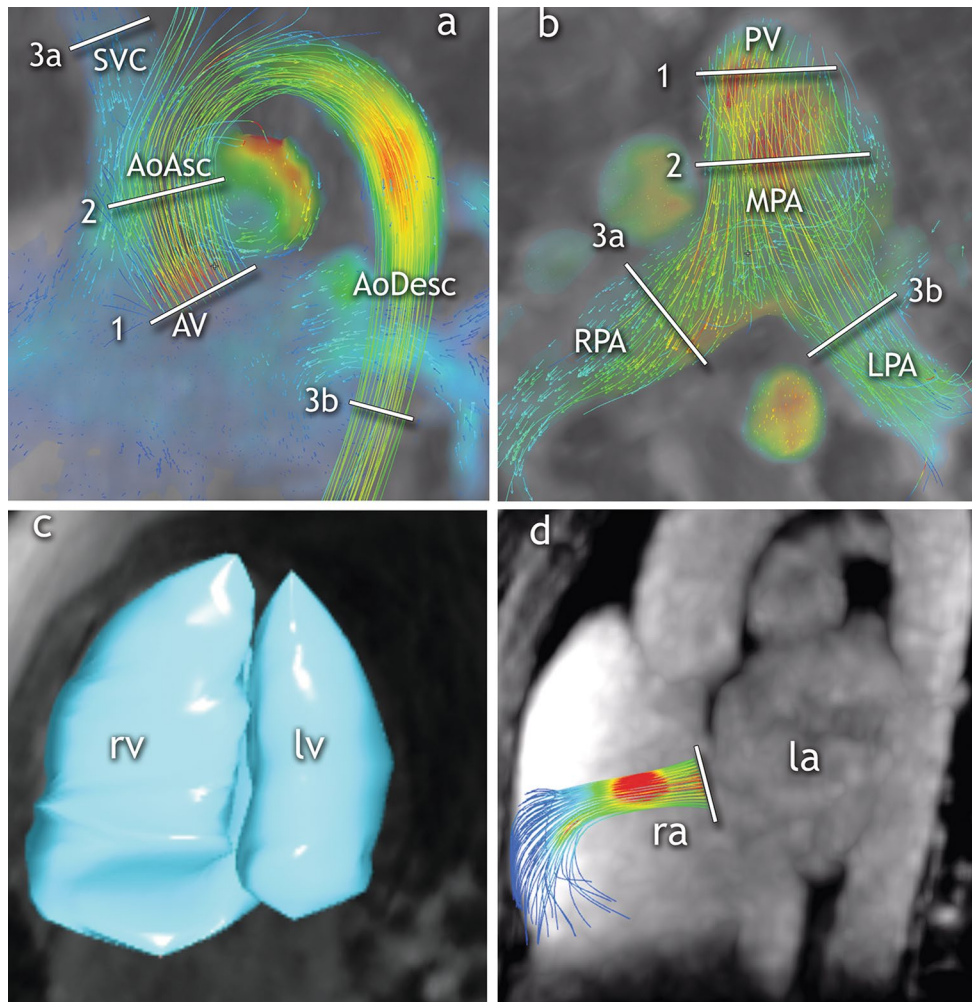


**Fig. 2** Levels of flow and shunt measurement. Systemic **a** and pulmonic **b** blood flows were measured at three different levels. Systemic flow **a** was measured at the aortic valve level [1], ascending aorta level [2] and as sum ( $3 = 3a + 3b$ ) of the flow of the superior vena cava above the azygos vein ( $3a$ ) and descending aorta ( $3b$ ). When present, left persistent superior vena cava flow was added to the sum

of SVC and descending aorta. Pulmonic flow **b** was measured at the pulmonary valve level [1], main pulmonary artery level [2] and as the sum of the right ( $3a$ ) and left pulmonary artery flow ( $3b$ ). Ventricular stroke volumes were calculated using magnitude images **c**. Additionally, shunt volumes were measured at the ASD level by septal tracking **d**

emphasize the flow across the atrial septum (Fig. 1). Incidental findings including the presence of a bicuspid aortic valve (BAV) and PAPVR were also documented.

#### Quantification of flow and of shunt

Management of ASD is mostly driven by the severity of cardiac shunting, defined by the pulmonary ( $Q_p$ ) and systemic ( $Q_s$ ) blood flow ratio [2, 5]. Three levels were used to obtain  $Q_p$  and  $Q_s$  flow: (1) valve, (2) main artery and (3) periphery (Fig. 2). The valve and vessels were tracked and “contoured” throughout the entire cardiac cycle [19].

Shunt fractions ( $Q_p/Q_s$ ) were calculated for each level in all patients.

Alternatively, ventricular stroke volume may be used for shunt fraction calculation, provided that no significant ( $\leq 20\%$ ) valve insufficiency is present. The study population was screened for valvular insufficiency, which was quantified if detected. In the subset of patients with no significant valvular insufficiency, the shunt fraction was calculated additionally using the right ventricular (RVSV) and left ventricular (LVSV) stroke volume ratio. For this, end-diastolic and end-systolic ventricular volumes were segmented from the 4D flow magnitude anatomic images [20]. Lastly, shunt

volumes were measured at the atrial level by tracking the atrial septum (Fig. 2). Indirect shunt volume quantification was obtained by subtracting systemic from pulmonary blood flow ( $Q_p - Q_s$ ).

## Statistics

Statistical analysis was performed with SPSS software version 21 (IBM, New York, USA) and GraphPad Prism 4 Project (San Diego, CA, USA). Categorical variables are presented as number and percentages and continuous variables as mean ( $\pm$  standard deviation) or median (minimum–maximum). Correlation between measurements at different levels was evaluated using Spearman's (rho) coefficient for nonparametric data, and agreement was analyzed with Bland-Altman plots [21]. The Spearman rho coefficient was classified as “very weak” for values of 0.00–0.19, “weak” for 0.20–0.39, “moderate” for 0.40–0.59, “strong” for 0.60–0.79 and “very strong” for 0.80–1.0 [22]. Interobserver reliability was assessed by intraclass correlation coefficient (ICC).

## Results

### Study population

Four-dimensional flow MRI examinations from 30 patients with ASD were gathered from the four academic centers. One nondiagnostic examination was excluded. (Supplementary Fig. 3). Mean age was 43 ( $\pm$  17) years, and 11 (38%) patients were male. Six patients had two ASDs, and one patient had four ASDs. Of the 38 ASDs, 26 (68%) were classified as secundum, 4 (11%) primum and 8 (21%) sinus venosus [6 at the SVC level, 1 at the inferior vena cava (IVC) level and 1 unroofed coronary sinus]. Additional findings included PAPVR ( $n=2$ ) and BAV ( $n=5$ ).

### Correlation of 4D blood flow and stroke volume measurements

Median  $Q_p$  was 8.5 l/min (4.4–20.2 l/min) at the main pulmonary artery level; 8.6 l/min (3.2–20.3 l/min) at the pulmonary valve level and 8.7 l/min (4.4–19.9 l/min) at the pulmonary branch level. Median cardiac output measured from RVSV was 9 l/min (4.6–20.0 l/min). The correlations between  $Q_p$  measurements performed at different levels were classified as very strong (Spearman's rho = 0.885–0.886) (Fig. 3). Pulmonary flow measured in the main pulmonary

artery also correlated well with right ventricular stroke volume (Spearman's rho = 0.972). Relative to the main pulmonary artery, measurements at pulmonary valve and pulmonary branches overestimated flow by 0.15 l/min and 0.27 l/min, respectively (Fig. 3), while RVSV overestimated with 0.26 l/min. Bland-Altman, ranges, and biases are presented in Table 2.

For systemic flow, median  $Q_s$  is 4.9 l/min (2.7–10.7 l/min) at the ascending aorta level, 5.2 l/min (2.9–10.0 l/min) at the aortic valve level and 4.7 l/min (2.9–10.5 l/min) at the peripheral level. Median cardiac output measured from LVSV was 4.8 l/min (3.0–8.2 l/min). Similarly, the correlations between  $Q_s$  measurements performed at different levels were classified as very strong (Spearman's rho = 0.991–0.974) (Table 2, Fig. 4). Relative to the ascending aorta results, measurements at the aortic valve overestimated  $Q_s$  with 0.14 l/min, and by 0.17 l/min at the peripheral level, while measurements of the LVSV underestimated  $Q_s$  with 0.16 l/min (Fig. 4). Bland-Altman, ranges, and biases are presented in Table 2.

### Correlation of 4D flow shunt fraction measurements

Good correlation was found between  $Q_p/Q_s$  ratios derived at the main artery level and ratios derived at the valve and peripheral level (Spearman's  $\rho = 0.95$  for both comparisons), with smaller bias for the valve level vs. peripheral level ( $-0.023$  l/min vs.  $-0.049$  l/min,  $p = 0.922$ ) (Supplementary Fig. 4). Bland-Altman, ranges, and biases are presented in Table 3. A threshold of 1.5 is often used as a threshold for ASD closure. In our cohort, 10 patients had ratios measuring below 1.5 at all levels, and 16 patients had shunt ratios measuring above 1.5 at all levels. In only three patients did we observe some measurements above and below the 1.5 threshold, and at all locations these measurements tended to stay close to 1.5 (range 1.3–1.7) (Fig. 5).

### Interobserver consistency of 4D flow, shunt fraction and volume measurements

Measurements of blood flow, shunt fraction and shunt volume with 4D flow were highly reproducible between two independent readers. Interobserver consistency for flow measurements was excellent at all levels, showing ICCs all  $\geq 0.955$ . Interobserver consistency for the calculated shunt fraction showed ICCs  $\geq 0.98$  and for shunt volume ICCs  $\geq 0.979$ . All ICCs for measurements of blood flow, calculated shunt fractions ( $Q_p/Q_s$ ) and shunt volumes are displayed in Table 4.

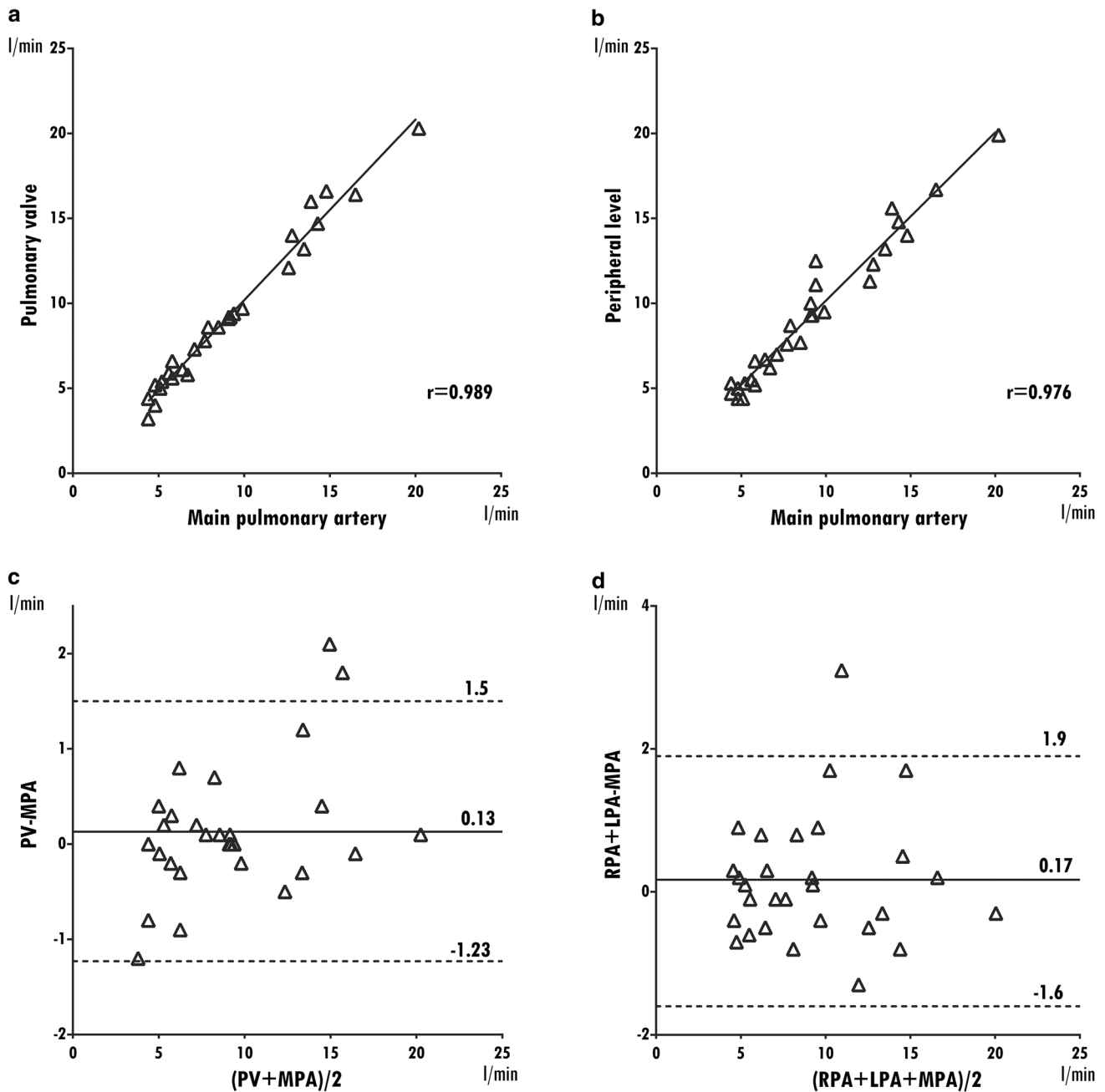


**Fig. 3** Pulmonary flow. Correlation and Bland-Altman plots of pulmonary flow measured at different levels using as reference the level of the main pulmonary artery. For each Bland-Altman plot, the average of measurements from both levels is plotted on the x-axis and the dif-

ference is plotted on the y-axis. The solid gray horizontal line plots the mean difference, and the dotted gray lines indicate the limits of agreement. *PV* pulmonary valve, *MPA* main pulmonary artery, *RPA* right pulmonary artery, *LPA* left pulmonary artery

### Direct versus indirect 4D shunt volume measurements

In 20/29 patients (69%), it was feasible to obtain direct shunt volumes at the exact location of the septal defect. Correlations between direct and indirect ( $Q_p - Q_s$ ) measurements

were classified as very strong (Spearman's  $\rho = 0.96$ ). However, shunt volume was underestimated by 0.57 l/min using direct measurements. Bland-Altman, ranges and standard deviation are presented in Table 5. Two of these patients had multiple ASDs, but some small ASDs did not allow for direct flow measurement (Supplementary Fig. 5).

**Table 2** Consistency of flow measurements at different locations

Level of measurement	Flow (l/min) median (min–max)	Spearman's rho <sup>a</sup>	Bland-Altman	
			Bias	± 1.96 SD
<b>Pulmonic flow</b>				
Pulmonary valve	8.6 (3.2–20.3)	0.886	0.148	–0.86 to 1.16
Main pulmonary artery	8.5 (4.4–20.2)	–	–	–
Right + left pulmonary arteries	8.7 (4.4–19.9)	0.885	0.266	–1.12 to 1.65
Right ventricular stroke volume <sup>b</sup>	9.0 (4.6–20.0)	0.972	–0.257	–2.01 to 1.49
<b>Systemic flow</b>				
Aortic valve	5.2 (2.9–10.0)	0.991	0.135	–1.23 to 1.5
Ascending aorta	4.9 (2.7–10.7)	–	–	–
SVC <sup>c</sup> + descending aorta	4.7 (2.9–10.5)	0.974	0.169	–1.6 to 1.94
Left ventricular stroke volume <sup>b</sup>	4.8 (3.0–8.2)	0.906	0.157	–2.45 to 2.1

Absolute blood flow measurements are consistent across multiple locations and with stroke volumes

SVC superior vena cava

<sup>a</sup>Main pulmonary artery and ascending aorta are taken as reference

<sup>b</sup>Eight patients had more than 20% mitral or tricuspid regurgitation and were excluded from the analysis

<sup>c</sup>SVC measured above the azygos vein when visible

## Discussion

We show in this study that 4D flow MRI can be sufficient for evaluation of patients with ASD, including quantification of shunt fraction, and can be robustly performed at multiple institutions; 4D flow MRI is consistent and reliable for measuring systemic and pulmonic blood flow and obtaining shunt fractions at multiple levels across the vascular tree. In daily practice, a shunt fraction ( $Q_p/Q_s$ ) threshold above 1.5 is often used as a critical parameter to determine the need for ASD closure. By 4D flow MRI, few patients had mixed results near the 1.5 threshold. In those patients, other clinical features may be used to decide upon individual surgical or medical management, such as right heart chamber enlargement or pulmonary pressure [2, 5].

In this study, direct shunt volume quantification was obtained at the level of ASD by tracking the atrial septum frame by frame throughout the cardiac cycle. Direct shunt volume quantification was feasible in 69% of the patients and correlated well with calculated shunt volumes obtained by 4D flow measurements at the level of main arteries ( $Q_p-Q_s$ ) ( $r=0.955$ ). Tracking the atrial septum may be challenging if there is insufficient image quality, if the size of the ASD is small or if there are multiple ASDs. For example, in two patients the direct quantification value was lower than the indirect quantification. When these cases were further reviewed, we found additional shunts, which were missed in the initial analysis (Supplementary Fig. 5). Therefore, we believe that direct quantification of each ASD can be helpful to determine whether all of shunts have been appropriately accounted for. Mismatch between direct and

indirect measurements may point to additional undetected shunts.

We show in the current study that it is possible to achieve excellent multilevel and interreader reproducibility with 4D flow MRI at multiple centers. This alleviates some previous concerns that 4D flow might only be achievable at one or two centers with extensive experience. This is further supported by recent studies showing good scan-rescan reproducibility and good intraobserver agreement with 4D flow [23, 24]. We further show here that experienced readers are not necessarily required to achieve high reproducibility. In addition, we demonstrate here that 4D flow can enable measurement of shunts at multiple alternative locations. This is especially helpful in the case of turbulent flow, aliasing or metallic artifacts. The 4D flow measurements can be performed at an alternative location distant to such artefacts to answer the clinical question. In patients with BAV, for example, flow acceleration across the aortic valve [25] can compromise the accuracy of measurements in areas of turbulent flow [26, 27], and an alternate measurement may be more accurate.

We present the current work, recognizing that 4D flow is an evolving imaging technique [28, 29] and new strategies are being developed, including incorporation of multiple velocity encoding speeds [30, 31]. To date, 4D flow has shown its potential for evaluation of congenital heart disease [32], and is being introduced in daily clinical practice for other clinical indications [33]. Additional work may be required to assess the performance of 4D flow in specific clinical scenarios. In the current work, we did not explore a direct comparison to other advanced imaging techniques, which can also be used to assess shunt fraction. For

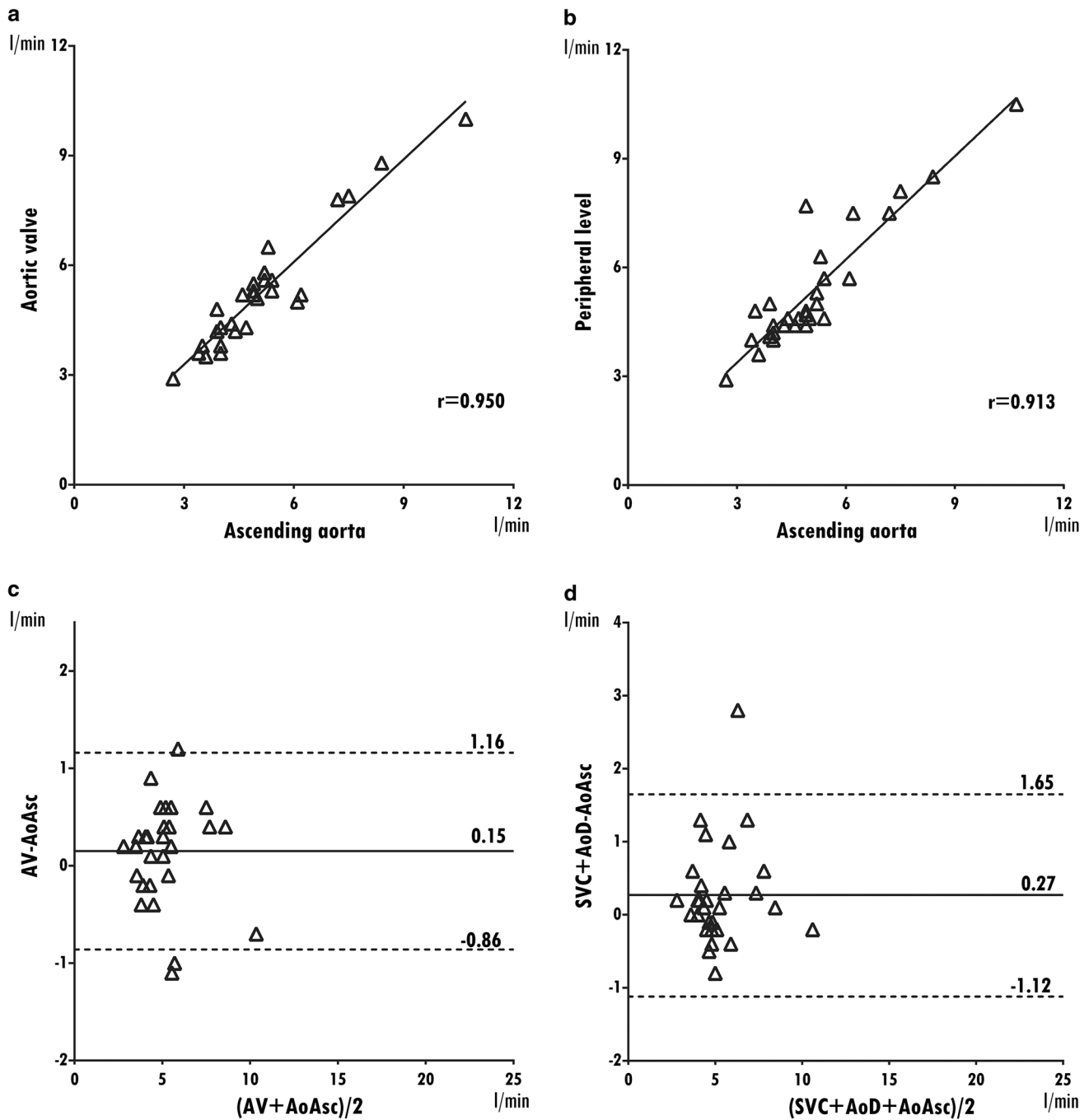


**Fig. 4** Systemic flow. Correlation and Bland-Altman plots of systemic flow measurements at different levels and taking as reference the level of the ascending aorta. For each Bland-Altman plot, the average of measurements from both levels is plotted on the x-axis and

the difference is plotted on the y-axis. The solid gray horizontal line plots the mean difference, and the dotted gray lines indicate the limits of agreement. *AV* aortic valve, *AoAsc* ascending aorta, *AoD* descending aorta, *SVC* superior vena cava

example, Yamasaki et al. propose CT as an approach for quantification of ASD [34], obtaining ventricular stroke volumes from finely detailed anatomic data. However, without flow information provided by 4D flow or echocardiography, this approach may be confounded by concomitant valve regurgitation.

## Limitations

We recognize a few potential limitations of the study. The patient population was not large, but we believe sufficient to demonstrate the robustness of the method. Second, although it is a study across multiple centers, all 4D flow acquisitions

**Table 3** Comparison of shunt fractions measured at different locations

Level of measurement	Shunt fraction median (min–max)	Spearman’s rho <sup>a</sup>	Bland-Altman	
			Bias	± 1.96 SD
Valve	1.6 (0.9–3.7)	0.95	–0.023	–0.42 to 0.37
Main artery <sup>a</sup>	1.6 (1.0–3.5)			
Peripheral	1.6 (0.8–3.9)	0.95	–0.049	–0.47 to 0.37
Stroke volume <sup>b</sup>	1.8 (1.0–3.3)	0.93	0.072	–0.57 to 0.71

<sup>a</sup>Level of main arteries is taken as reference

<sup>b</sup>Eight patients had more than 20% mitral or tricuspid regurgitation and were excluded from the analysis

**Fig. 5** Distribution of atrial septal defect shunt fractions ( $Q_p/Q_s$ ) measured at multiple levels.  $Q_p/Q_s$  at different locations ordered from high to low. A solid line is placed at the treatment threshold of 1.5  $Q_p/Q_s$ . Arrows highlight the three patients in which the measurements at different levels are crossing the threshold line

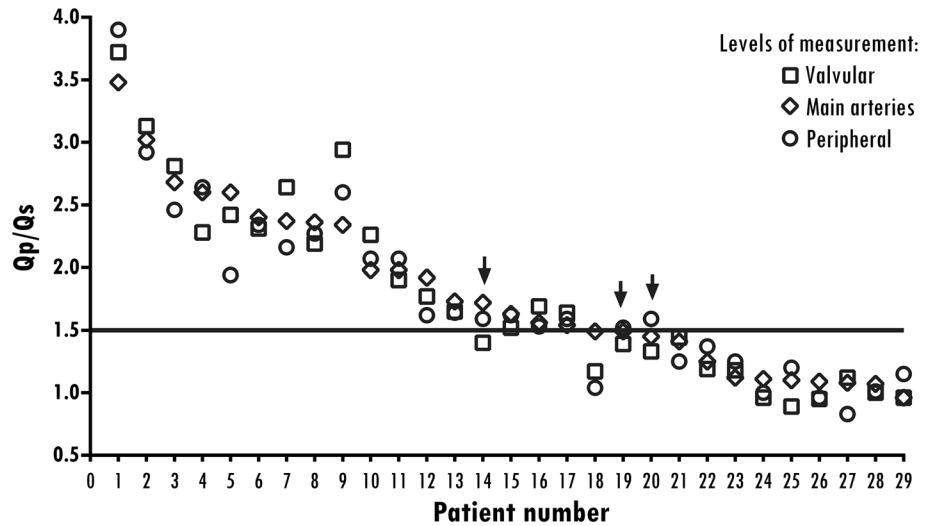


**Table 4** Comparison of flow measurements by independent observers

Level	Systemic flow	Pulmonary flow	$Q_p/Q_s$	Shunt volume
Valve	0.968	0.987	0.983	0.989
Main artery	0.975	0.986	0.981	0.987
Peripheral	0.955	0.981	0.968	0.979

Intraclass coefficients (ICCs) for measurements of blood flow, calculated shunt fractions ( $Q_p/Q_s$ ) and shunt volumes displayed

were performed using equipment from a single vendor. Additional work may be required to confirm similar quality 4D flow measurements can be obtained on other platforms. Third, a gadolinium-based contrast agent was used prior

to image acquisition at all sites. Further work is needed to determine whether similar results can be obtained without intravenous contrast. In addition, we did not perform a direct comparison against 2D phase-contrast MRI in this study. We did find that flow measurements were consistent with stroke volumes obtained from anatomical data, which was reassuring. Multiple previous studies have compared 4D flow and 2D phase-contrast measurements, showing that measurements from each technique are generally consistent [35, 36]. Bollache and colleagues showed better correlation between 4D flow and three-direction-velocity 2D phase-contrast than with the one-direction-velocity 2D phase-contrast technique, which is the most commonly used clinical technique [36].

**Table 5** Comparison of shunt volume measured at the atrial septal level against measurement at the main artery level

Level of measurement	Shunt volume (l/min) median (min–max)	Spearman’s rho <sup>†</sup>	Bland-Altman	
			Bias (l/min)	± 1.96 SD
Atrial septum <sup>∞</sup>	2.95 (0.2–8.7)	0.955	–0.57	–2.71 to 1.57
Main artery <sup>†</sup>	3.6 (–0.2 to 1.8)	–	–	–

<sup>∞</sup>Direct measurement of ASD was feasible in 20 patients

<sup>†</sup>Level of main arteries is taken as reference

## Conclusions

For patients referred for evaluation of ASD, 4D flow MRI showed excellent multilevel and interreader reproducibility for systemic and pulmonary blood flow measurements and shunt quantification obtained at different levels throughout the vascular tree.

**Funding** This study was funded by a grant from the Dutch Heart Foundation (The Hague, The Netherlands, grant no. 2013T093) and GE Healthcare.

## Compliance with ethical standards

**Conflict of interest** R.G. Chelu received funding for research from GE Healthcare and is a consultant to Arterys, Inc. J.W. Roos-Hessellink received a grant from the Dutch Heart Foundation. K. Nieman reports non-financial support from Siemens Medical Solutions and grants from GE Healthcare and Bayer Healthcare, outside the submitted work. S.S. Vasanawala is involved in research collaboration with GE Healthcare, is founder of and consultant to Arterys, Inc., and received a research grant from Bayer AG. A. Hsiao is founder of and consultant to Arterys, Inc., and received a research grant from GE Healthcare. The rest of the authors report no conflict of interest.

**Ethical standards** Patient studies were aggregated from multiple centers and approved by each local IRB, including either a waiver of consent or prospective enrollment with signed consent, as deemed appropriate by each center. The study protocol was compliant with the Declaration of Helsinki.

**Open Access** This article is distributed under the terms of the Creative Commons Attribution 4.0 International License (<http://creativecommons.org/licenses/by/4.0/>), which permits unrestricted use, distribution, and reproduction in any medium, provided you give appropriate credit to the original author(s) and the source, provide a link to the Creative Commons license, and indicate if changes were made.

## References

1. Van Der Linde D, Konings EEM, Slager MA et al (2011) Birth prevalence of congenital heart disease worldwide: a systematic review and meta-analysis. *J Am Coll Cardiol Elsevier Inc* 58(21):2241–2247. <https://doi.org/10.1016/j.jacc.2011.08.025>
2. Baumgartner H, Bonhoeffer P, De Groot NMS et al (2010) ESC Guidelines for the management of grown-up congenital heart disease (new version 2010). *Eur Heart J* 31(23):2915–2957
3. Roos-Hessellink JW, Meijboom FJ, Spitaels SEC et al (2003) Excellent survival and low incidence of arrhythmias, stroke and heart failure long-term after surgical ASD closure at young age. A prospective follow-up study of 21–33 years. *Eur Heart J* 24(2):190–197. <http://www.ncbi.nlm.nih.gov/pubmed/12573276>. Accessed Feb 27 2017
4. Cuypers JAAE, Opić P, Menting ME et al (2013) The unnatural history of an atrial septal defect: longitudinal 35 year follow up after surgical closure at young age. *Heart BMJ Publ Group Ltd British Cardiovascular Soc* 99(18):1346–1352. <http://www.ncbi.nlm.nih.gov/pubmed/23886606>. Accessed Feb 24 2017
5. Warnes CA, Williams RG, Bashore TM et al (2008) ACC/AHA 2008 Guidelines for the management of adults with congenital heart disease: a report of the American College of Cardiology/American Heart Association task force on practice guidelines (writing committee to develop guidelines on the management of a. *Circulation* 118(23):e714–e833. <http://www.ncbi.nlm.nih.gov/pubmed/18997169>. Accessed December 2, 2014
6. Roest AA, Helbing WA, van der Wall EE, de Roos A (1999) Postoperative evaluation of congenital heart disease by magnetic resonance imaging. *J Magn Reson Imaging* 10(5):656–666. <http://www.ncbi.nlm.nih.gov/pubmed/10548773>. Accessed June 28 2017
7. Beerbaum P, Parish V, Bell A, Gieseke J, Körperich H, Sarikouch S (2008) Atypical atrial septal defects in children: noninvasive evaluation by cardiac MRI. *Pediatr Radiol* 38(11):1188–1194. <http://www.ncbi.nlm.nih.gov/pubmed/18787816>. Accessed June 28 2017
8. Valsangiacomo Buechel ER, Grosse-Wortmann L, Fratz S, et al (2015) Indications for cardiovascular magnetic resonance in children with congenital and acquired heart disease: an expert consensus paper of the Imaging Working Group of the AEPC and the cardiovascular magnetic resonance section of the EACVI. *Cardiol Young* 1–20. [http://www.journals.cambridge.org/abstract\\_S1047951115000025](http://www.journals.cambridge.org/abstract_S1047951115000025)
9. Thomson LEJ, Crowley AL, Heitner JF et al (2008) Direct en face imaging of secundum atrial septal defects by velocity-encoded cardiovascular magnetic resonance in patients evaluated for possible transcatheter closure. *Circ Cardiovasc Imaging* 1(1):31–40
10. Beerbaum P, Körperich H, Gieseke J, Barth P, Peuster M, Meyer H (2003) Rapid left-to-right shunt quantification in children by phase-contrast magnetic resonance imaging combined with sensitivity encoding. *Circulation* 108(11):1355–1361
11. Vasanawala SS, Hanneman K, Alley MT, Hsiao A (2015) Congenital heart disease assessment with 4D flow MRI. *J Magn Reson Imaging* 4. <https://doi.org/10.1002/jmri.24856>. <http://www.ncbi.nlm.nih.gov/pubmed/25708923>. (Epub 2015 Feb 24)
12. Hsiao A, Lustig M, Alley MT et al (2012) Rapid pediatric cardiac assessment of flow and ventricular volume with compressed sensing parallel imaging volumetric cine phase-contrast MRI. *AJR Am J Roentgenol* 198(3):W250–W259
13. Hanneman K, Kino A, Cheng JY, Alley MT, Vasanawala SS, Hospital TG (2016) Assessment of the precision and reproducibility of ventricular volume, function and mass measurements with ferumoxylol enhanced 4D flow MRI. *J Magn Reson Imaging* 44(2):383–392. <https://www.ncbi.nlm.nih.gov/pmc/articles/PMC4947013/pdf/nihms772886.pdf>
14. Stoll VM, Loudon M, Eriksson J et al (2018) Test-retest variability of left ventricular 4D flow cardiovascular magnetic resonance measurements in healthy subjects. *J Cardiovasc Magn Reson* 20(1):15. <https://doi.org/10.1186/s12968-018-0432-4>
15. Hanneman K, Sivagnanam M, Nguyen ET et al (2014) Magnetic resonance assessment of pulmonary ( $Q_p$ ) to systemic ( $Q_s$ ) flows using 4D phase-contrast imaging: pilot study comparison with standard through-plane 2D phase-contrast imaging. *Acad Radiol Elsevier Ltd* 21(8):1002–1008. <http://dx.doi.org/10.1016/j.acra.2014.04.012>. Accessed June 23 2015
16. Valverde I, Simpson J, Schaeffter T, Beerbaum P (2010) 4D phase-contrast flow cardiovascular magnetic resonance: comprehensive quantification and visualization of flow dynamics in atrial septal defect and partial anomalous pulmonary venous return. *Pediatr Cardiol* 31:1244–1248
17. Hsiao A, Yousaf U, Alley MT et al (2015) Improved quantification and mapping of anomalous pulmonary venous flow with four-dimensional phase-contrast MRI and interactive streamline rendering. *J Magn Reson Imaging*. <http://www.ncbi.nlm.nih.gov/pubmed/25914149>. Accessed June 5 2015

18. Tariq U, Hsiao A, Alley M, Zhang T, Lustig M, Vasanawala SS (2013) Venous and arterial flow quantification are equally accurate and precise with parallel imaging compressed sensing 4D phase contrast MRI. *J Magn Reson Imaging* 37(6):1419–1426. <http://www.pubmedcentral.nih.gov/articlerender.fcgi?artid=3582745&tool=pmcentrez&rendertype=abstract>. Accessed Sept 21 2015
19. Chelu RG, Wanambiro KW, Hsiao A et al (2016) Cloud-processed 4D CMR flow imaging for pulmonary flow quantification. *Eur J Radiol Elsevier Ireland Ltd* 85(10):1849–1856. <http://dx.doi.org/10.1016/j.ejrad.2016.07.018>
20. Hanneman K, Kino A, Cheng JY, Alley MT, Vasanawala SS, Hospital TG (2016) Assessment of the precision and reproducibility of ventricular volume, function and mass measurements with ferumoxytol enhanced 4D flow MRI. *J Magn Reson Imaging* 44(2):383–392
21. Martin Bland J, Altman D (1986) Statistical methods for assessing agreement between two methods of clinical measurement. *Lancet* 327(8476):307–310. <http://linkinghub.elsevier.com/retrieve/pii/S0140673686908378>. Accessed Feb 27 2017
22. Spearman's correlation. <http://www.statstutor.ac.uk/resources/uploaded/spearman.pdf>. Accessed Aug 22 2017
23. Markl M, Wallis W, Harloff A. Reproducibility of flow and wall shear stress analysis using flow-sensitive four-dimensional MRI. *J Magn Reson Imaging*. 2011;33(4):988–994. <http://www.ncbi.nlm.nih.gov/pubmed/21448968>. Accessed June 28 2017
24. van Ooij P, Powell AL, Potters WV, Carr JC, Markl M, J and BA (2016) Reproducibility and interobserver variability of systolic blood flow velocity and 3D wall shear stress derived from 4D flow MRI in the healthy aorta. *J Magn Reson Imaging*. 43(1):236–248. <http://www.ncbi.nlm.nih.gov/pubmed/26140480>. Accessed Sept 5 2017
25. Bissell MM, Hess AT, Biasioli L et al (2013) Aortic dilation in bicuspid aortic valve disease: flow pattern is a major contributor and differs with valve fusion type. *Circ Cardiovasc Imaging* 6(4):499–507. <http://www.pubmedcentral.nih.gov/articlerender.fcgi?artid=3859916&tool=pmcentrez&rendertype=abstract>. Accessed Dec 13 2014
26. Hsiao A, Alley MT, Massaband P, Herfkens RJ, Chan FP, Vasanawala SS (2011) Improved cardiovascular flow quantification with time-resolved volumetric phase-contrast MRI. *Pediatr Radiol* 41(6):711–720
27. Brien KRO, Myerson SG, Cowan BR, Young AA, Robson MD (2009) Phase contrast ultrashort te: a more reliable technique for measurement of high-velocity turbulent stenotic jets. *Magn Reson Med* 63(6):626–636
28. Callaghan FM, Grieve SM (2016) Spatial resolution and velocity field improvement of 4D-flow MRI. *Magn Reson Med*. <http://www.ncbi.nlm.nih.gov/pubmed/27885707>. Accessed June 28 2017
29. Stalder AF, Russe MF, Frydrychowicz A, Bock J, Hennig J, Markl M (2008) Quantitative 2D and 3D phase contrast MRI: optimized analysis of blood flow and vessel wall parameters. *Magn Reson Med* 60(5):1218–1231. <http://www.ncbi.nlm.nih.gov/pubmed/18956416>. Accessed June 28 2017
30. Ha H, Kim GB, Kweon J, et al (2016) Multi-VENC acquisition of four-dimensional phase-contrast MRI to improve precision of velocity field measurement. *Magn Reson Med* 75(5):1909–1919. <http://doi.wiley.com/10.1002/mrm.25715>. Accessed June 28 2017
31. Callaghan FM, Kozor R, Sherrah AG et al (2016) Use of multi-velocity encoding 4D flow MRI to improve quantification of flow patterns in the aorta. *J Magn Reson Imaging* 43(2):352–363. <http://doi.wiley.com/10.1002/jmri.24991>. Accessed June 28 2017
32. Lawley CM, Broadhouse KM, Callaghan FM, Winlaw DS, Figtree GA, Grieve SM (2017) 4D flow magnetic resonance imaging: role in pediatric congenital heart disease. *Asian Cardiovasc Thorac Ann* 218492317694248. <http://journals.sagepub.com/doi/10.1177/0218492317694248>. Accessed June 28 2017
33. Kanski M, Töger J, Steding-Ehrenborg K et al (2015) Whole-heart four-dimensional flow can be acquired with preserved quality without respiratory gating, facilitating clinical use: a head-to-head comparison. *BMC Med Imaging* 15(1):20. <http://www.ncbi.nlm.nih.gov/pubmed/26080805>. Accessed June 28 2017
34. Yamasaki Y, Nagao M, Kawanami S et al (2017) One-stop shop assessment for atrial septal defect closure using 256-slice coronary CT angiography. *Eur Radiol* 27(2):697–704. <http://www.ncbi.nlm.nih.gov/pubmed/27236816>. Accessed Feb 20 2017
35. Kamphuis VP, van der Palen RLF, de Koning PJH et al (2017) In-scan and scan-rescan assessment of LV in- and outflow volumes by 4D flow MRI versus 2D planimetry. *J Magn Reson Imaging*. <http://doi.wiley.com/10.1002/jmri.25792>. Accessed Sept 5 2017
36. Bollache E, van Ooij P, Powell A, Carr J, Markl M, Barker AJ (2016) Comparison of 4D flow and 2D velocity-encoded phase contrast MRI sequences for the evaluation of aortic hemodynamics. *Int J Cardiovasc Imaging* 32(10):1529–1541. <http://link.springer.com/10.1007/s10554-016-0938-5>. Accessed June 28 2017